Supporting Information

New 2D Cu-MOF Constructed from Carboxylate Ligand Containing C-H···π Interaction as a Recyclable Responsive Luminescent Sensor for VOCs Vapors

*Chengxin Liu,[a] Jin Cui,[*b] Yufang Wang[c] and Mingjie Zhang[*a]*

a. Department of Chemistry, School of Sciences, Tianjin University, Tianjin 30035, P. R. of China.

b. National Foodstuff Inspection Center, Tianjin Product Quality Inspection Technology Research Institute, Tianjin 300384, P. R. of China.

c. Scientific Research Department, Shijiazhuang University of Applied Technology, Shijiazhuang 050081, P. R. of China.

General Considerations

Unless otherwise noted, all reactions were performed with oven-dried glassware with chemicals or reagents obtained from commercial sources. Solvents were dried over 4-8 Å mesh molecular sieves (Aldrich). Reactions were monitored by thin layer chromatography on 0.20 mm Anhui Liangchen silica gel plates and spots were detected with UV light. Silica gel (200-300 mesh) (from Qingdao ocean Chemical Plant) was used for flash chromatography. NMR data were collected on a Bruker AVANCE III HD 400-MHz NMR Spectrometer. Infrared spectroscopy was recorded with an ALPHA spectrophotometer at room temperature. Elemental analyses were determined in house using an elementar vario el III elemental analyzer. Thermal analyses were performed in nitrogen in the temperature range 25–800 °C with a heating rate of 10 °C min^{-1} on a Netzsch TG 209 F3 instrument. Powder X-ray diffraction patterns were obtained on a D/MAX-2500 of Rigaku Corporation Powder Diffractometer at a scan rate of 5°/min^{-1}. Fluorescence spectra, the fluorescence absolute quantum yields (Φfl) and time-resolved fluorescence measurements were recorded on a Fluorolog-3 of HORIBA Jobin Yvon spectrofluorometer. The images of compound **6**, Cu-MOF and activated Cu-MOF were taken under the Leica-DMI1 inverted biological microscope. The dynamic vapor adsorption was texted in dynamic vapor adsorption apparatus of TA-Instrument-VTI-SA+. Surface area and pore size distribution measurements were measured using a Micromeritics ASAP 2020 surface area and pore size analyzer. Before the measurements, activated Cu-MOF (100 mg) was degassed under reduced pressure at 100 °C for 10 h. Pore size distribution data were calculated from the N_2 sorption isotherms at 77 K based on non-local density functional theory (NLDFT) model in the Micromeritics ASAP2020 software package (assuming slit pore geometry). The data of X-ray crystallography was collected on a XtaLAB mini (600W, SHINE, CCD, 75mm, 0.1 electrons/pisel/sec) X-ray single crystal diffractometer. The structure was solved and refined by direct methods using the SHELXS 97 program.[1,2] The non-hydrogen atoms were refined using anisotropic thermal parameters. All the hydrogen atoms were located at geometrically calculated positions.

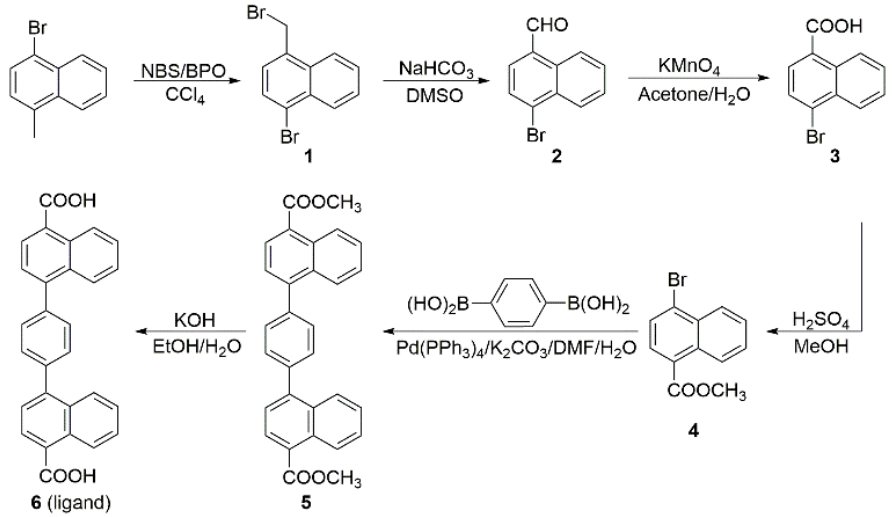

Figure S1. Synthesis of ligand (compound **6**).

The ligand was synthesized in good yields using 1-bromo-4-methylnaphthalene as the starting material. 1-Bromo-4-methylnaphthalene was treated with N-bromosuccinimide and dibenzoyl peroxide with CCl_4 as solvent to obtain compound **1**. Compound **1** was heated with $NaHCO_3$ in DMSO to give compound **2** as yellow solid. Then compound **2** was refluxed in acetone and oxidized by $KMnO_4$ to give compound **3**, which was subsequently refluxed with sulfuric acid in MeOH to obtain compound **4**. Refluxing of compound **4** with 1,4-Phenylenebisboronic acid, tetrakis-(triphenylphosphine)-palladium and K_2CO_3 in DMF and H_2O gave compound **5**, which then refluxed with 10% NaOH and ethyl alcohol generated compound **6**.

Synthesis of 1-bromo-4-(bromomethyl)naphthalene (compound 1) [3]

A 500 mL Schlenk flask was added 1-bromo-4-methylnaphthalene (10 g, 48 mmol, 1 eq), N-bromosuccinimide (9.4 g, 53 mmol, 1.1 eq), dibenzoyl peroxide (1 g, 4 mmol, 0.083 eq) and CCl_4 (150 mL). After refluxed for 5 h under N_2 atmosphere, the mixture was cooled to room temperature and filtered, the write precipitate was wash by CCl_4 (100 mL) for three times. Then the resulting filtrate was washed by saturated sodium sulfite solution (200 mL), dried over anhydrous sodium sulfate, and achieved by flash chromatography on a silica gel column (aether petrolei). the resulting write solid product was dried in vacuum at room temperature. Yield: 71 %. ^{1}H NMR (400 MHz, Chloroform-d) δ 8.21 (d, *J* = 7.9 Hz, 1H), 8.04 (d, *J* = 8.0 Hz, 1H), 7.61 (d, *J* = 7.6 Hz, 1H), 7.55 (t, *J* = 7.5 Hz, 2H), 7.26 (d, *J* = 7.6 Hz, 1H), 4.80 (s, 2H). ^{13}C NMR (100 MHz, Chloroform-d) δ 133.36, 132.45, 132.14, 129.55, 128.15, 127.91, 127.67, 127.43 , 124.59, 124.27, 30.99.

Synthesis of 4-bromo-1-naphthaldehyde (compound 2)[3]

A 250 mL flask was charged with compound **1** (4.5 g, 15 mmol, 1 eq,) $NaHCO_3$ (2.5 g, 30 mmol, 2 eq) and DMSO (50 mL). The mixture was heated to 95ºC for 5 h. After cooling to room temperature, ice water (100 mL) was added. The mixture was extracted with ethyl acetate (3 x 100 mL). Further purification of the resulting yellow solid product was achieved by flash chromatography (10 % ethyl acetate in aether petrolei). Yield: 62 %.^{1}H NMR (400 MHz, Chloroform-d) δ 10.34 (s, 1H), 9.26 (d, *J* = 8.3 Hz, 1H), 8.34 (d, *J* = 7.9 Hz, 1H), 7.94 (d, *J* = 7.7 Hz, 1H), 7.77 (d, *J* = 7.7 Hz, 1H), 7.75–7.63 (m, 2H). ^{13}C NMR (100 MHz, Chloroform-d) δ 192.63, 136.13, 132.14, 131.43, 131.34, 130.9, 129.81, 129.36, 128.30, 127.74, 125.14.

Synthesis of 4-Bromo-1-naphthalenecarboxylic acid (compound 3) [3]

Compound **2** (5 g, 21 mmol, 1 eq) and acetone (50 mL) was refluxed in a 250 mL round bottom flask equipped with a stir bar. $KMnO_4$ (6 g, 38 mmol, 1.8 eq) in water (100 mL) was added dropwise to the boiling mixture for 3 h and continue refluxed for 2 h. Then the mixture was filtered at a high temperature. The black precipitate was wash by acetone (50 mL) and water (50 mL). The acetone was removed in vacuum and the water solution was washed by saturated sodium sulfite solution (50 mL) and diethyl ether (50 mL). The colorless transparent solution was cooled to 0ºC and adjusted to pH 1.0 with 1 M HCl, the resulting white precipitate was collected by filtration, washed by hot water and dried in vacuum at 110 ºC. Yield: 85 %. ^{1}H NMR (400 MHz, DMSO-d6) δ 13.47 (s, 1H), 9.02–8.86 (m, 1H), 8.27 (dd, *J* = 7.4, 2.7 Hz, 1H), 8.10–7.94 (m, 2H), 7.77 (dd,

J = 6.6, 3.3 Hz, 2H). ^{13}C NMR (100 MHz, DMSO-d6) δ 168.53, 132.24, 131.81, 130.49, 129.85, 128.96, 128.72, 128.55, 127.48, 127.41, 126.71.

Synthesis of methyl 4-bromo-1-naphthoate (compound 4)

Compound **3** (3 g, 12 mmol) was dissolved in a mixed solution of MeOH (90 mL) and concentrated sulfuric acid (3 mL) refluxed for 12 h in a 250 mL round bottom flask. After cooling to room temperature, the mixture was concentrated in vacuum and extracted with CH_2Cl_2 (3 x 30 mL). The organic layer was dried over Na_2SO_4, filtered and concentrated in vacuo to give the resulting product pale yellow oil. Yield: 92 %. ^{1}H NMR (400 MHz, Chloroform-d) δ 8.91–8.81 (m, 1H), 8.28–8.19 (m, 1H), 7.89 (d, *J* = 7.9 Hz, 1H), 7.72 (d, *J* = 7.9 Hz, 1H), 7.56 (td, *J* = 7.5, 6.3, 4.2 Hz, 2H), 3.91 (s, 3H). ^{13}C NMR (100 MHz, Chloroform-d) δ 167.45, 132.40, 132.19, 130.11, 128.91, 128.82, 128.50, 127.71, 127.63, 126.99, 126.26, 52.37.

Synthesis of 1,4-bis(methyl 1-naphthoate)benzene (compound 5)

Under N_2 atmosphere, a 250 mL flask was charged with compound **4** (3 g, 12 mmol, 2.2 eq), 1,4-Phenylenebisboronic acid (0.9 g, 5.4 mmol, 1 eq), K_2CO_3 (1.1g, 8.1 mmol, 1.5 eq), tetrakis-(triphenylphosphine)-palladium (0.6 g, 0.8 mmol, 0.1 eq), DMF (60 mL) and H_2O (15 mL). The mixture was heated to 65ºC for 24 h. After cooling to room temperature, quantity of water was added. The mixture was filtrated and the filtrate was extracted with CH_2Cl_2 (3 x 80 mL). Further purification of the resulting write oil product was achieved by flash chromatography on a silica gel column (10 % ethyl acetate in aether petrolei). Yield: 69 %. ^{1}H NMR (400 MHz, Chloroform-d) δ 9.02 (d, *J* = 8.6 Hz, 1H), 8.27 (d, *J* = 7.5 Hz, 1H), 8.08 (d, *J* = 8.5 Hz, 1H), 7.69–7.64 (m, 1H), 7.63 (s, 2H), 7.56 (d, *J* = 7.4 Hz, 2H). ^{13}C NMR (100 MHz, Chloroform-d) δ 168.04, 144.87, 139.69, 132.08, 131.82, 129.94, 129.63, 127.64, 126.75, 126.66, 126.42, 126.13, 125.84, 52.28.

Synthesis of 1,4-bis(4-naphthoic acid)benzene (ligand, complex 6)

A suspension of compound **5** (2.5 g, 5.6 mmol) in 10% NaOH (40 mL) and ethyl alcohol (120 mL) was refluxed for 5 h in a 500 mL round bottom flask equipped with a stir bar. After cooling to room temperature, the mixture was concentrated in vacuum and acidized with 1 M HCl, white precipitate was collected by filtration, washed by hot water and dried in vacuum at 110ºC. Yield: 91 %. ^{1}H NMR (400 MHz, DMSO-d6) δ 13.27 (s, 1H), 9.02 (d, *J* = 8.6 Hz, 1H), 8.26 (d, *J* = 7.4 Hz, 1H), 8.04 (d, *J* = 8.5 Hz, 1H), 7.76–7.70 (m, 1H), 7.69 (s, 2H), 7.64 (t, *J* = 8.0 Hz, 2H). ^{13}C NMR (101 MHz, DMSO-d6) δ 169.10, 144.09, 139.50, 131.78, 131.66, 130.36, 129.77, 128.03, 127.94, 127.13, 126.61, 126.56, 126.45. FT-IR (cm^{-1}): 391 (w), 541 (w), 518 (w), 649 (w), 650 (w), 671 (w), 770 (m), 795 (w), 843 (w), 923 (w), 999 (w), 1105 (w), 1160 (w), 1189 (w), 1245 (m), 1271 (m), 1309 (w), 1325 (w), 1383 (w), 1430 (w), 1453 (w), 1504 (w), 1582(m), 1683(s), 2554 (w), 2664 (w), 2990 (m), 3424 (w). Elemental analysis (% calc/found: C 78.52/80.37, H 4.26/4.34).

Preparation of Cu-MOF

Compound **6** (21 mg, 0.05 mmol), TEA (14 μL) and DMF (2 mL) were stirred for 0.5 h in a 10 mL vial, then, $Cu(NO_3)_2$•$3H_2O$ (72mg, 0.3 mmol) was added. The vial was tightly capped, placed in an oven and heated to 110 °C in 4 h, held for 72 h, and then cooled to 25°C in 42.5 h to give 8 mg Cu-MOF as green transparent olivary crystal. Or,

compound **6** (21 mg, 0.05 mmol), HCl (5 μL) and DMF (2 mL) were stirred for 10 min in a 10 mL vial, then, $Cu(NO_3)_2 \cdot 3H_2O$ (72mg, 0.3 mmol) was added. The vial was tightly capped and placed in the same conditions to yield 8 mg of Cu-MOF as green transparent cuboid crystal. These two differently shaped crystals have the same unit cell parameters. FT-IR (cm^{-1}): 384 (w), 472 (w), 557 (w), 584 (w), 654 (w), 665 (w), 770 (m), 795 (w), 858 (w), 925 (w), 1001 (w), 1067 (w), 1089 (w), 1155 (w), 1245 (w), 1371 (m), 1391 (m), 1453 (w), 1505 (w), 1584 (w), 1606 (m), 1672 (m), 2334 (vw), 2357 (vw), 2839 (vw), 2951 (w). Elemental analysis (% calc/found: C 64.49/65.22, H 5.20/4.83, N 4.81/4.47).

Preparation of activated Cu-MOF

The obtained crystals of Cu-MOF were soaked in MeOH for 3 days at room temperature. The supernatant was decanted and fresh MeOH was added every day. Then the crystals were treated with CH_2Cl_2 for another 3 days similarly. After that, the mixture was filtered and the resulting green precipitate was heated in vacuum at 80°C for 3 h to remove the residual reagents in the pores. FT-IR (cm^{-1}): 391 (w), 480 (w), 584 (w), 669 (w), 770 (m), 795 (w), 843 (w), 850 (w), 925 (w), 1020 (w), 1040 (w), 1130 (w), 1158 (w), 1245 (w), 1370 (m), 1391 (m), 1453 (w), 1504 (w), 1582 (w), 1660 (m), 1672 (w), 2909 (w), 3018 (w), 3424 (m). Elemental analysis (% calc/found: C 68.49/70.07, H 3.57/3.36).

Preparation of activated Cu-MOF⊃guests

A 1.5 mL vial was charged with 15 mg activated Cu-MOF which had heated to 100°C in vacuum for 8 h. The vial was then placed into a 15 mL sealed container, which contains 3 mL testing solvent, for 48 h in 40°C. Subsequently the vial was taken out of the container and the emission spectra of activated Cu-MOF⊃guests was taken.

Figures

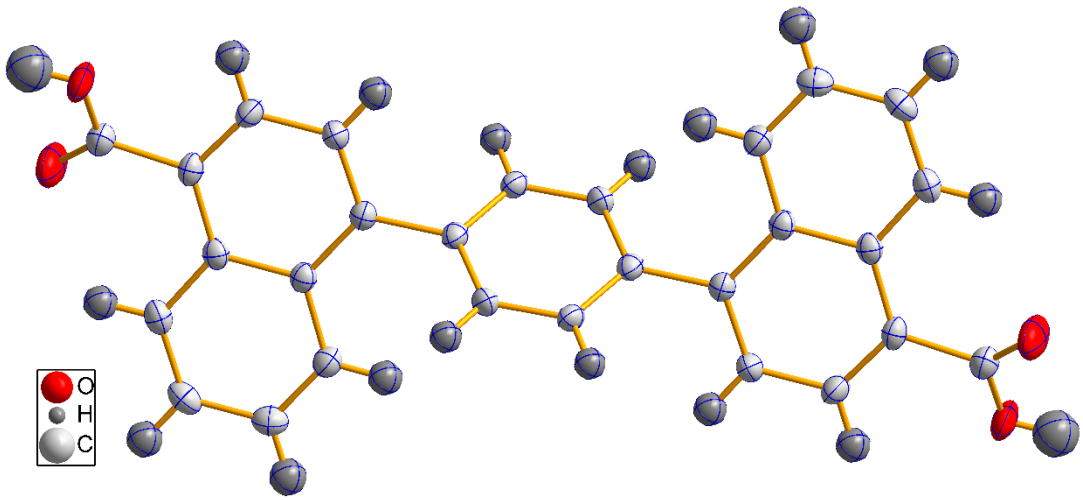

Figure S2. Structure of crystallographically independent molecules of ligand, the solvent molecules have been removed for clarity.

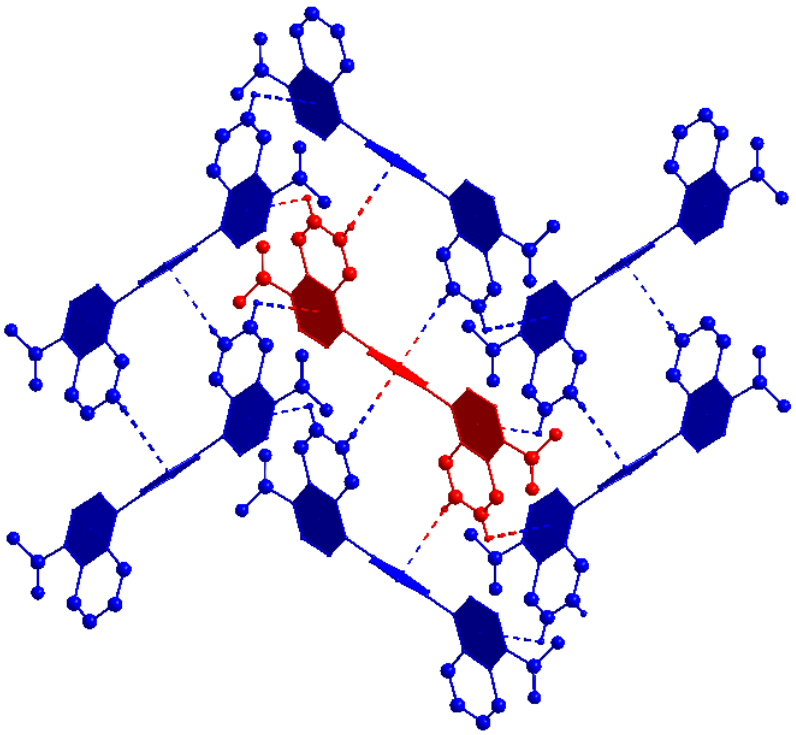

Figure S3. C–H···π interactions in a single ligand crystal, represented as dotted lines, measured between H and the adjacent phenyl ring centroids.

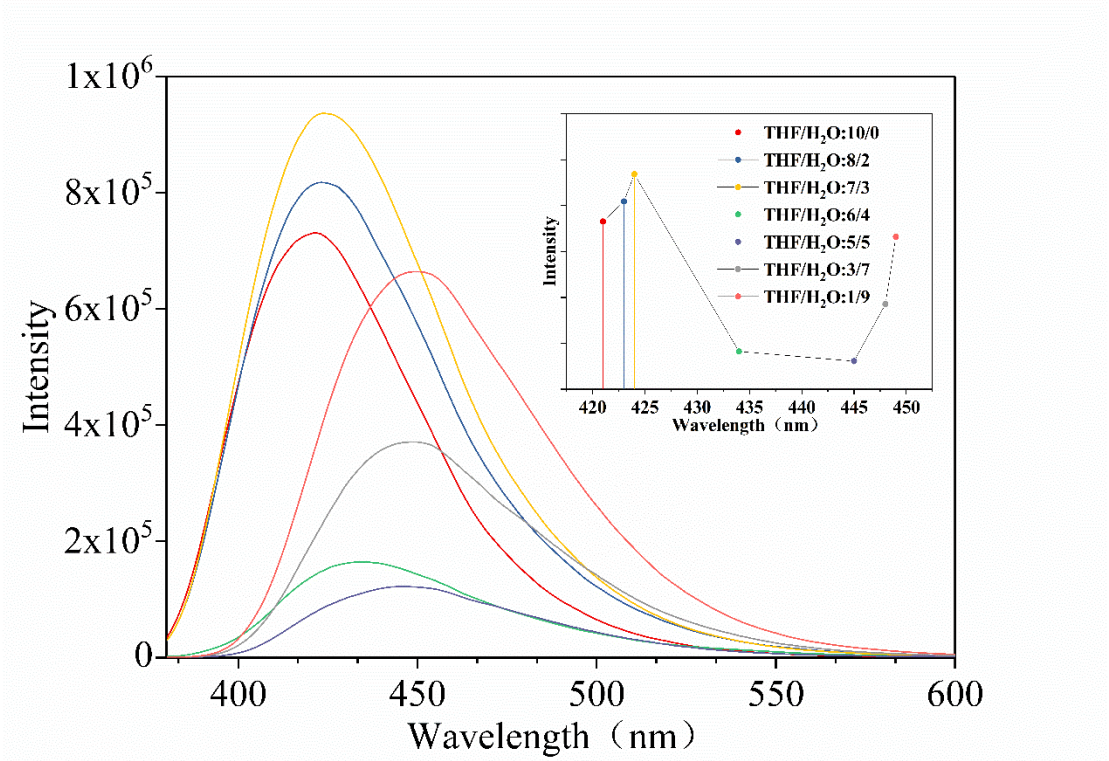

Figure S4. Fluorescence emission spectrum of the ligand in the THF/H_2O mixed solvent at various volume ratios. The inset: diagram of the changes in the intensity of fluorescence as a function of maximum emission.

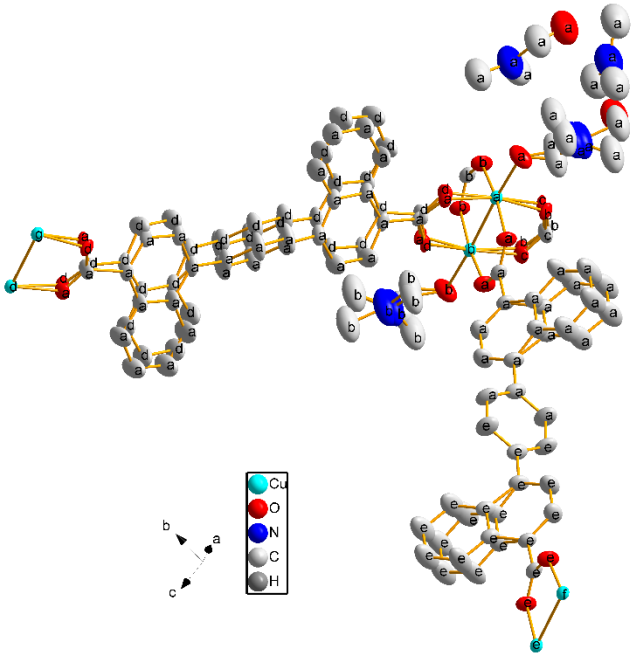

Figure S5. Unit-cell content of the crystal structure of Cu-MOF. Hydrogen atoms have been removed for clarity. Here, a = x, y, z; b = 1-x, 1-y, -z; c = x, -1+y, -1+z; d = 1-x, 2 -y, 1-z; e = 2-x, - y, 1-z; f = 2-x, -y, 1-z; g = x, 1+y, 1+z.

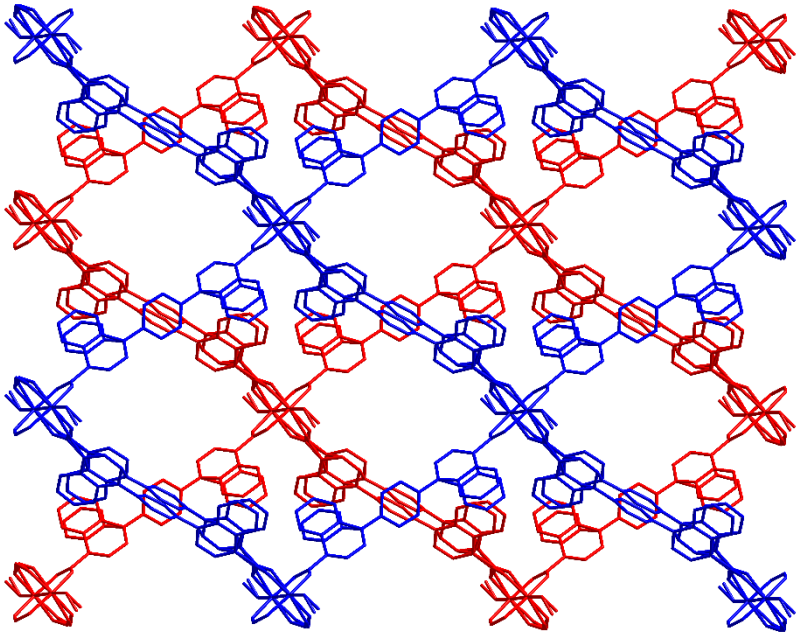

Figure S6. The crystal structure of Cu-MOF viewed along the [100] direction. Here, red and blue represent two neighboring layers. The solvent molecules have been removed for clarity.

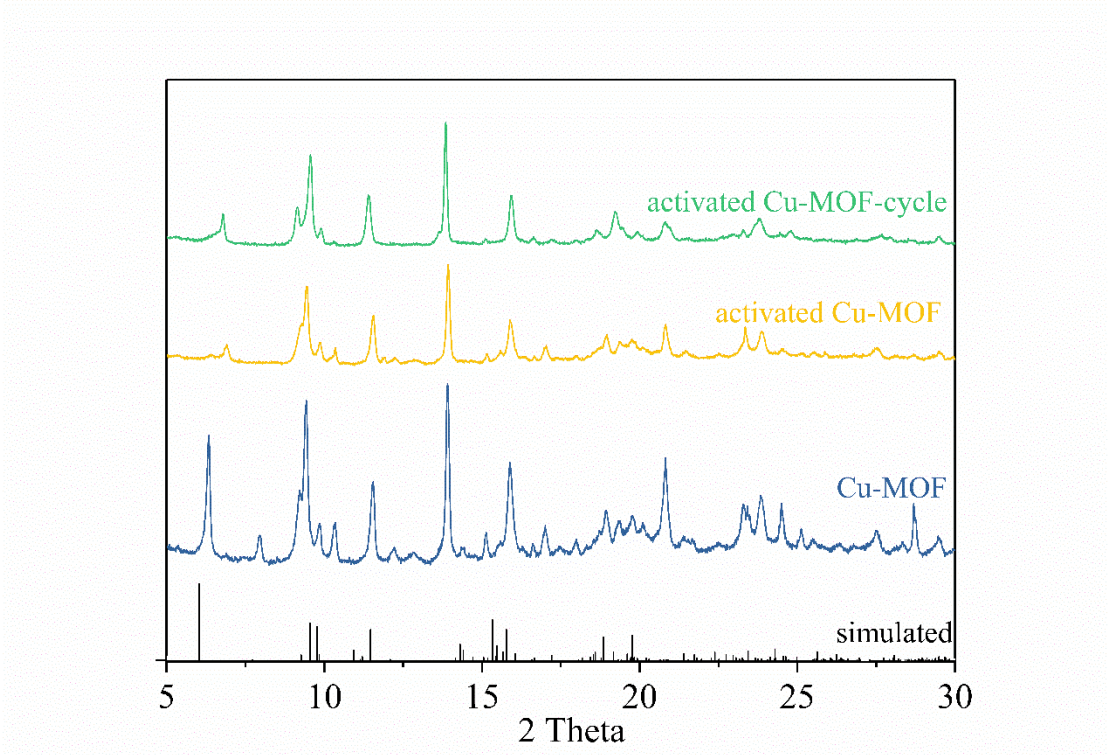

Figure S7. Simulated PXRD of Cu-MOF and measured PXRD of Cu-MOF, activated Cu-MOF and the activated Cu-MOF after cycle experiment.

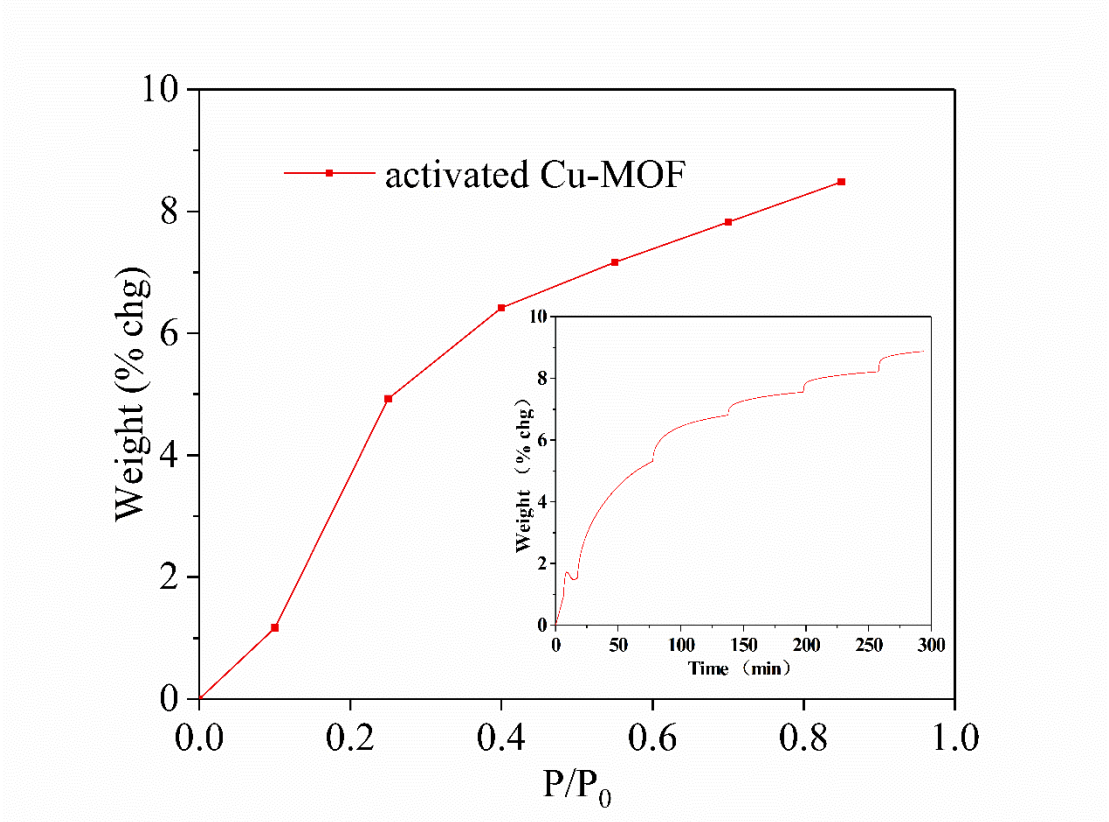

Figure S8. Dynamic vapor adsorption (VTI) of the activated Cu-MOF using benzene at room temperature. The inset: the weight changes as a function of time.

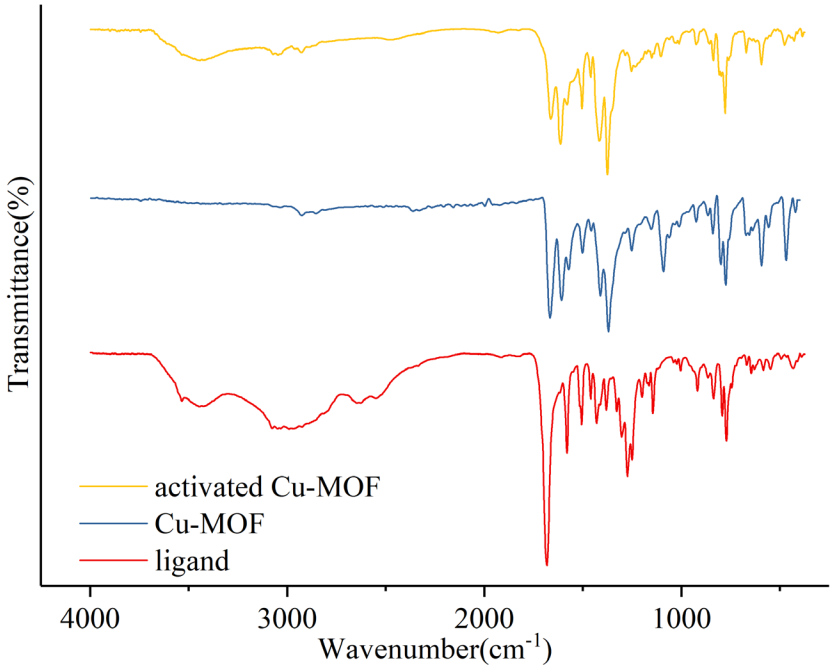

Figure S9. FT-IR spectra of ligand, Cu-MOF and activated Cu-MOF.

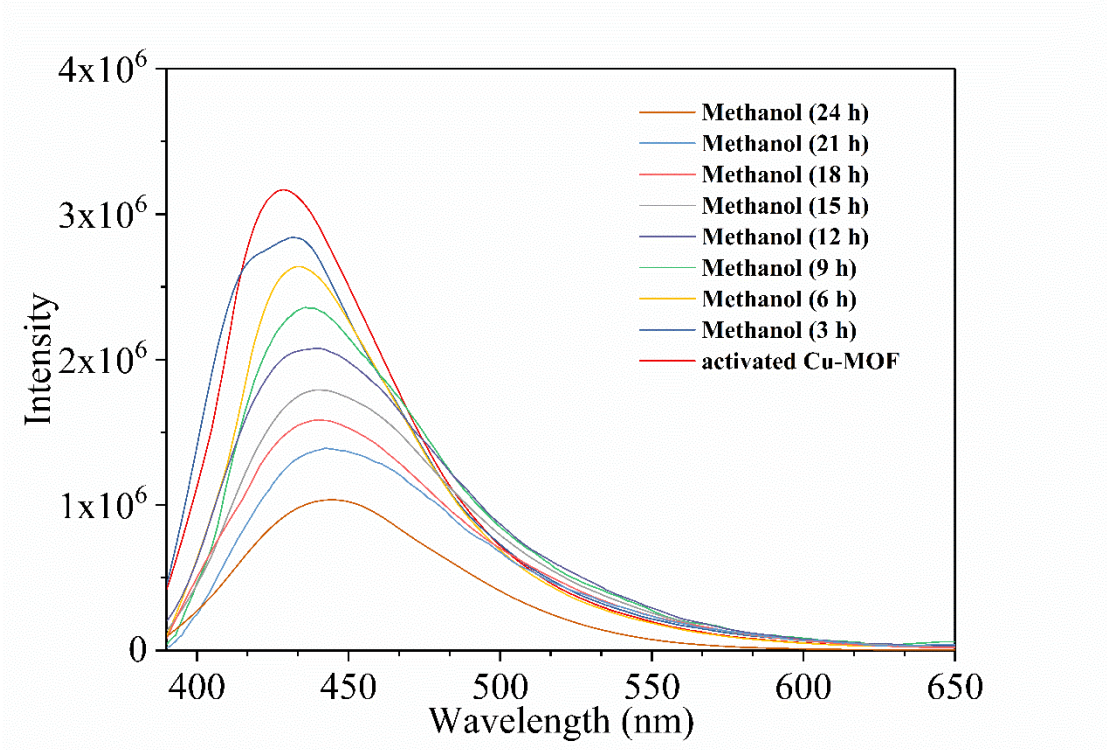

Figure S10. Changes in the intensity and emission spectrum of fluorescence with activated Cu-MOF exposed to methanol vapor.

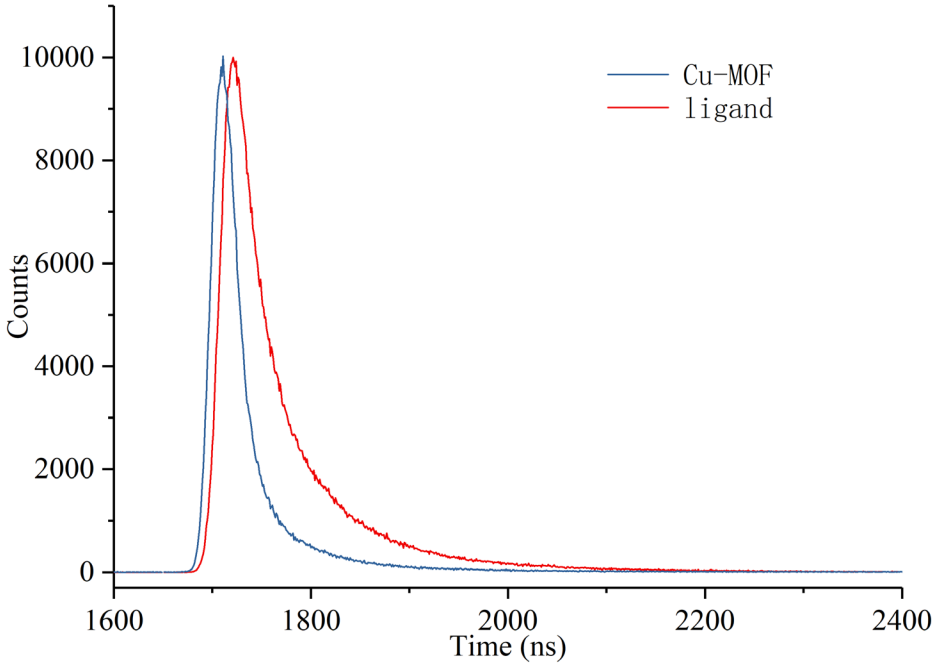

Figure S11. The fluorescence decay lifetime of ligand and Cu-MOF.

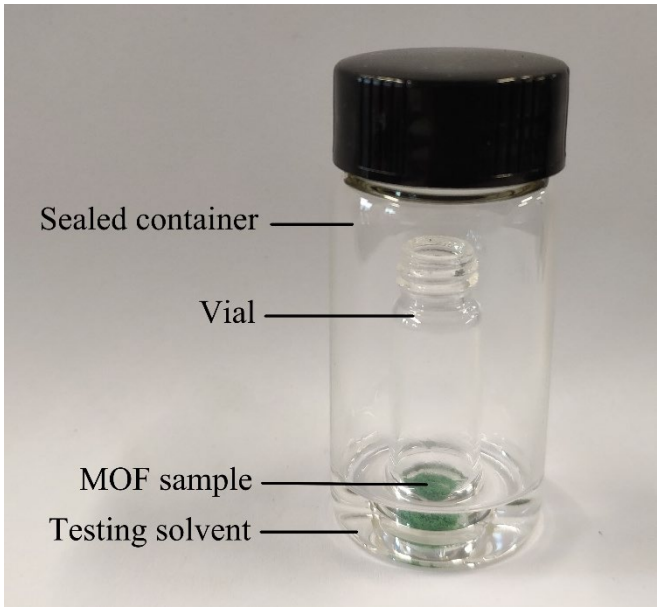

Figure S12. Diagram of the experimental setup for incubating activated Cu-MOF under different VOCs vapors.

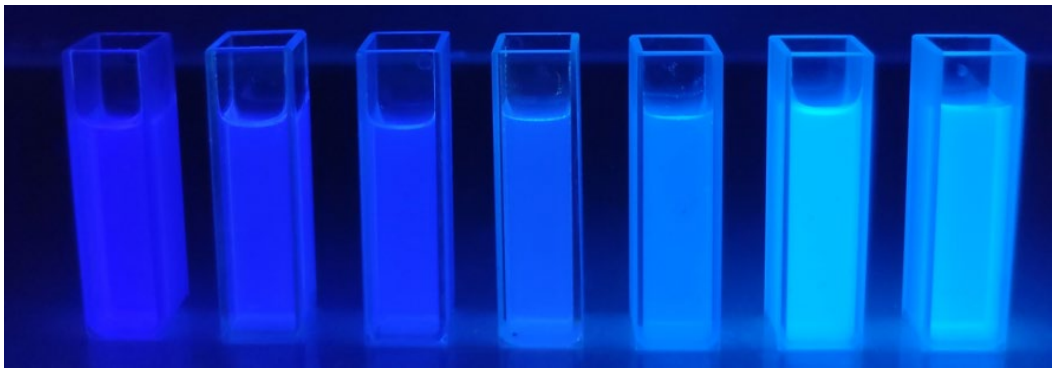

Figure S13. Fluorescent images of ligand in THF/H_2O mixed solvents with different volume ratios.

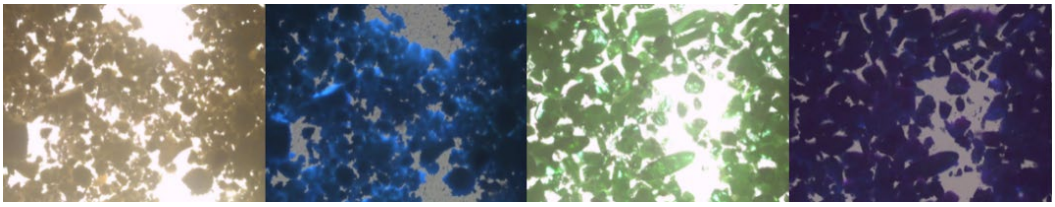

Figure S14. From left to right: under optical images of ligand, under fluorescent images of ligand, under optical images of Cu-MOF, under fluorescent images of Cu-MOF.

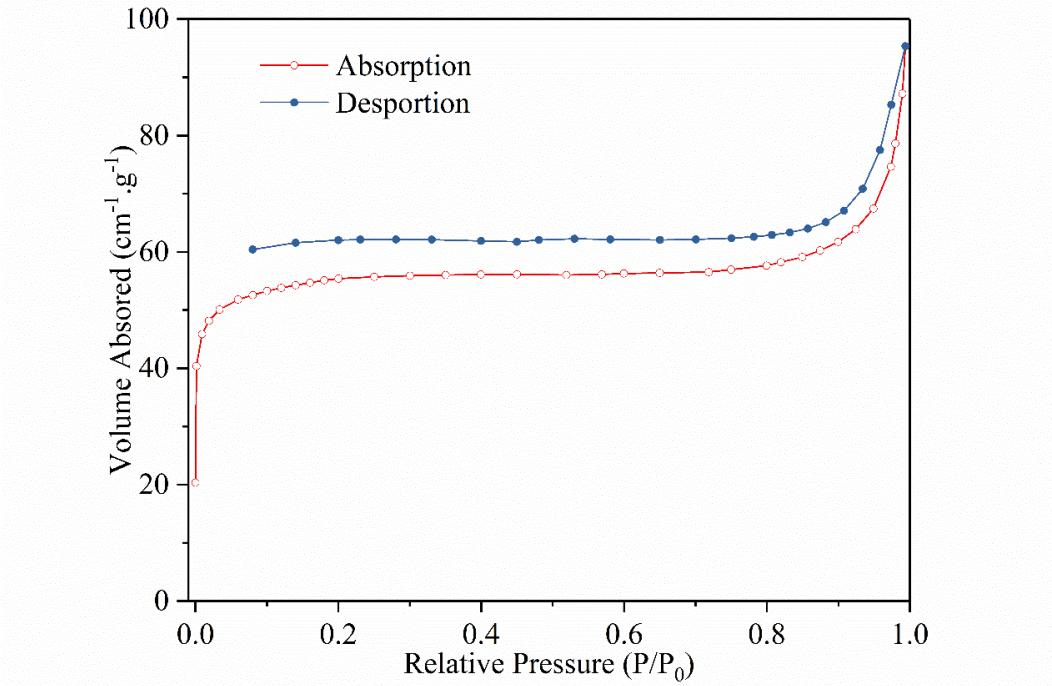

Figure S15. Nitrogen adsorption–desorption isotherm of activated Cu-MOF after the cyclic experiments.

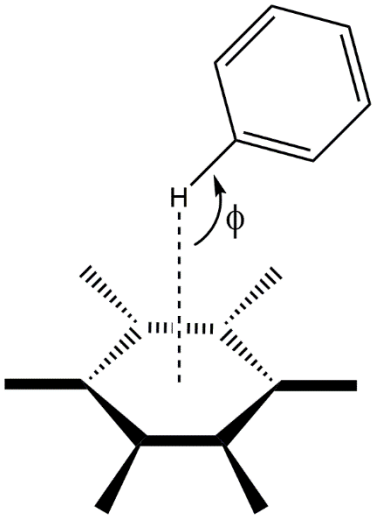

Figure S16. Orientation dependence of the C–H···π interactions.

Table S1. The distance (Å) and angle ϕ (°) of C–H···π interactions in Cu-MOF.

Entry	Bond	Distance	Angle
I a	C28-H··· π	3.1731(7)	142.265(712)
I b	C31-H··· π	2.9133(6)	153.744(698)
II a	C39-H··· π	3.3278(9)	148.503(863)
II b	C22-H··· π	2.8168(7)	131.870(901)
III a	C6-H··· π	3.2883(11)	139.609(923)
III b	C6A-H··· π	3.1798(13)	124.347(891)

NMR spectroscopy

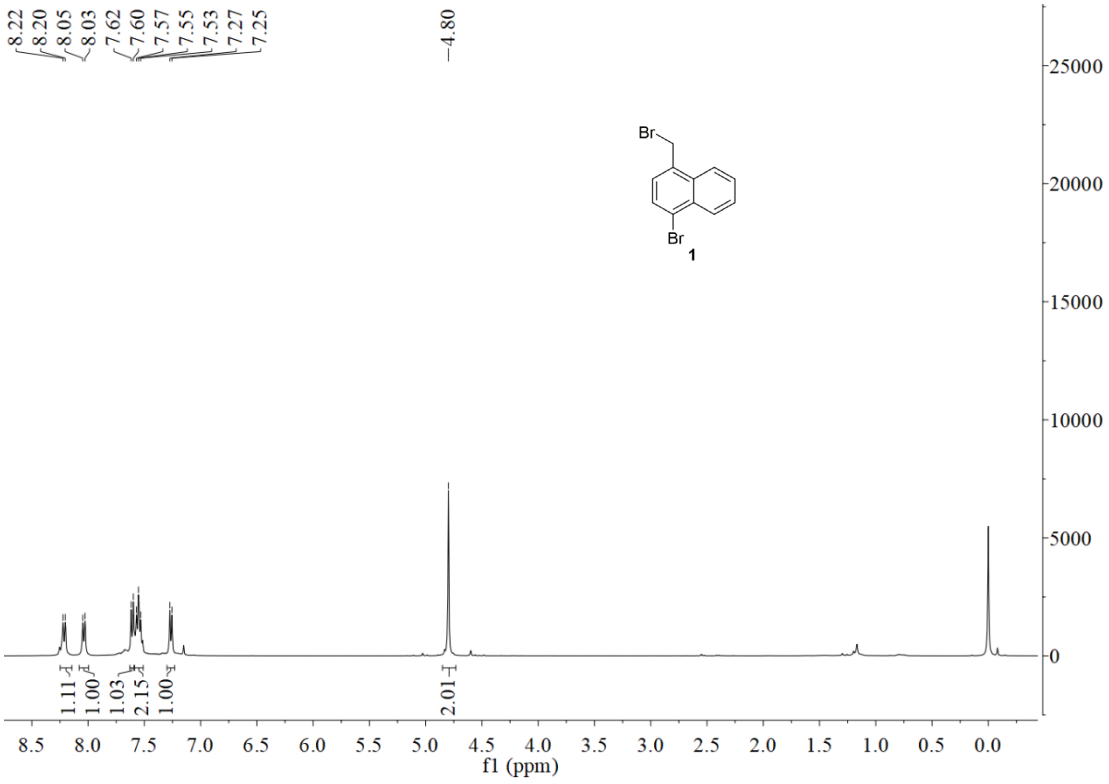

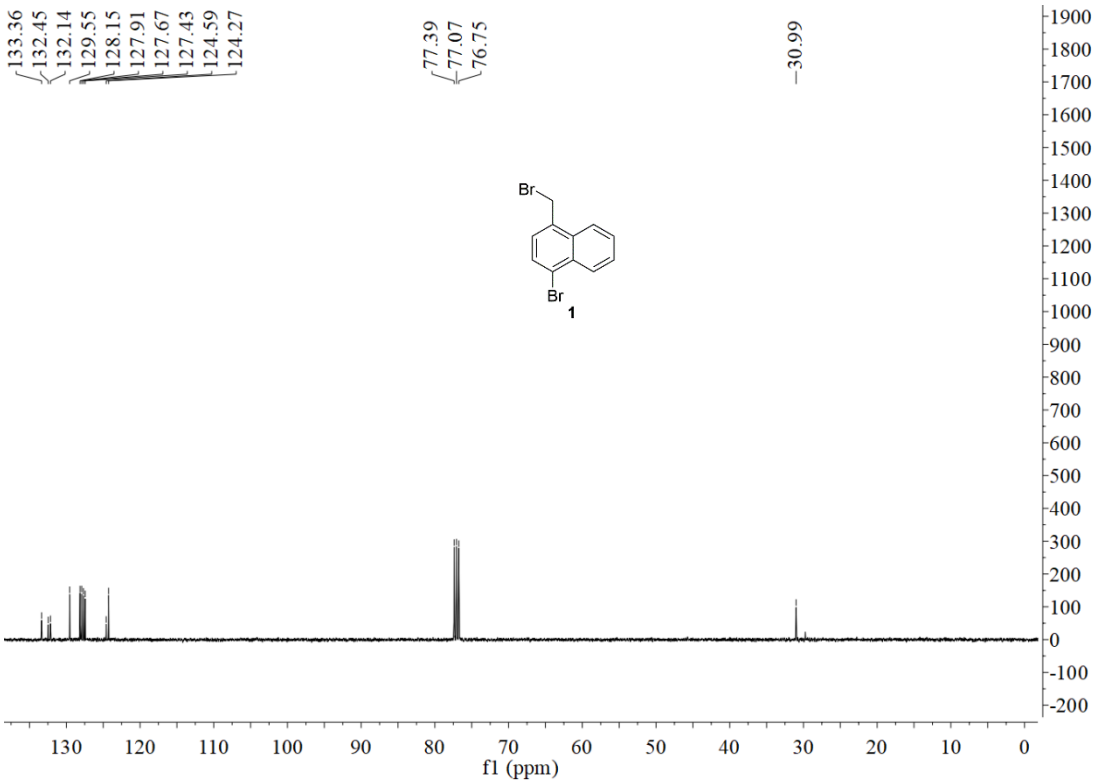
133.36
132.45
132.14
129.55
128.15
127.91
127.67
127.43
124.59
124.27
77.39
77.07
76.75
30.99
Br
Br
1
f1 (ppm)

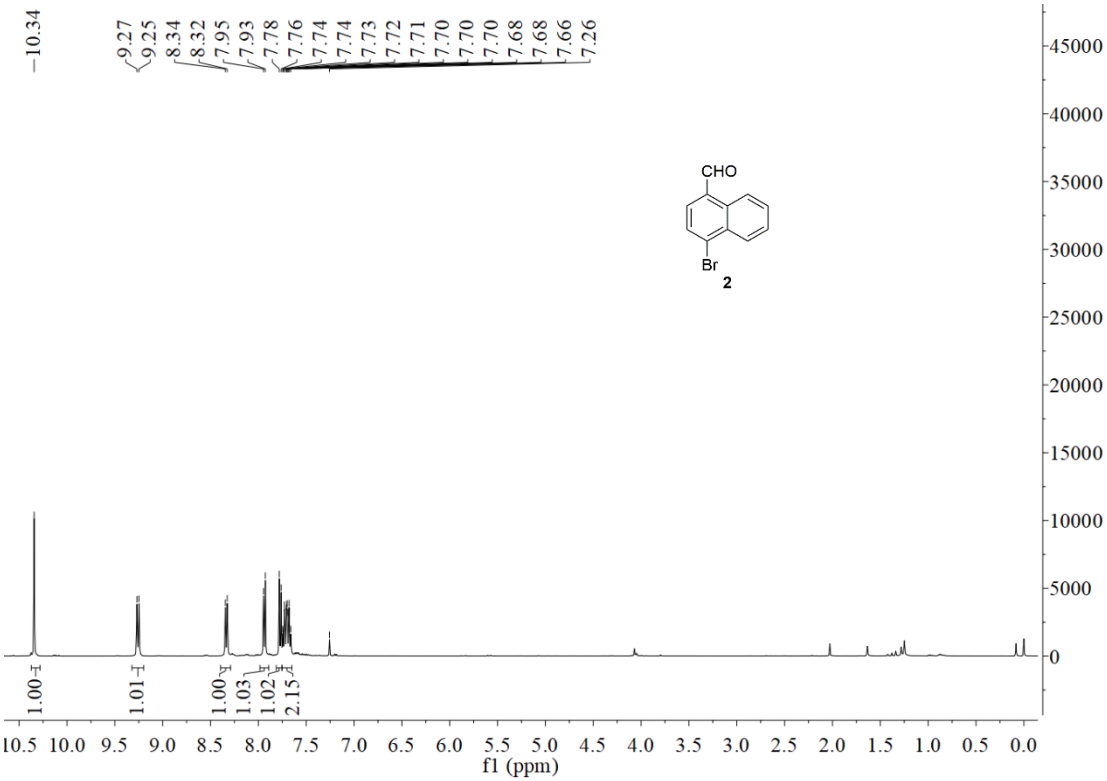
10.34
9.27
9.25
8.34
8.32
7.95
7.93
7.78
7.76
7.74
7.74
7.73
7.72
7.71
7.70
7.70
7.70
7.68
7.68
7.66
7.26
CHO
Br
2
1.00
1.01
1.00
1.03
1.02
2.15
f1 (ppm)

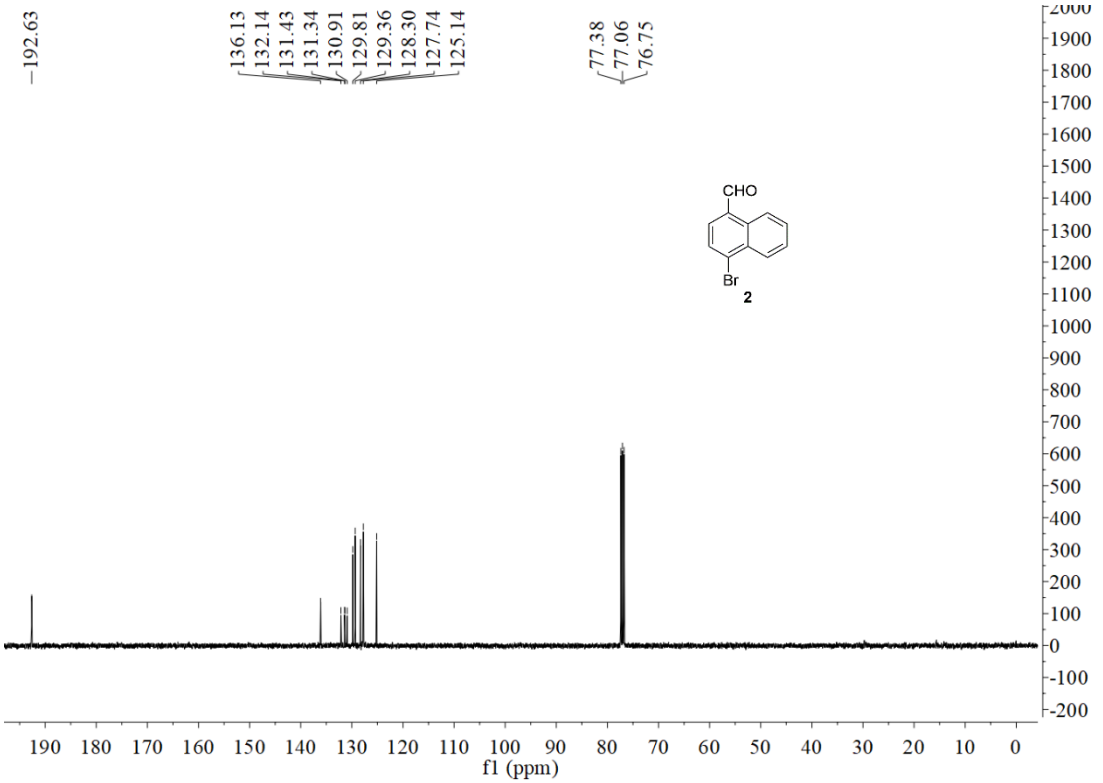
192.63
136.13
132.14
131.43
131.34
130.91
129.81
129.36
128.30
127.74
125.14
77.38
77.06
76.75
CHO
Br
2
f1 (ppm)

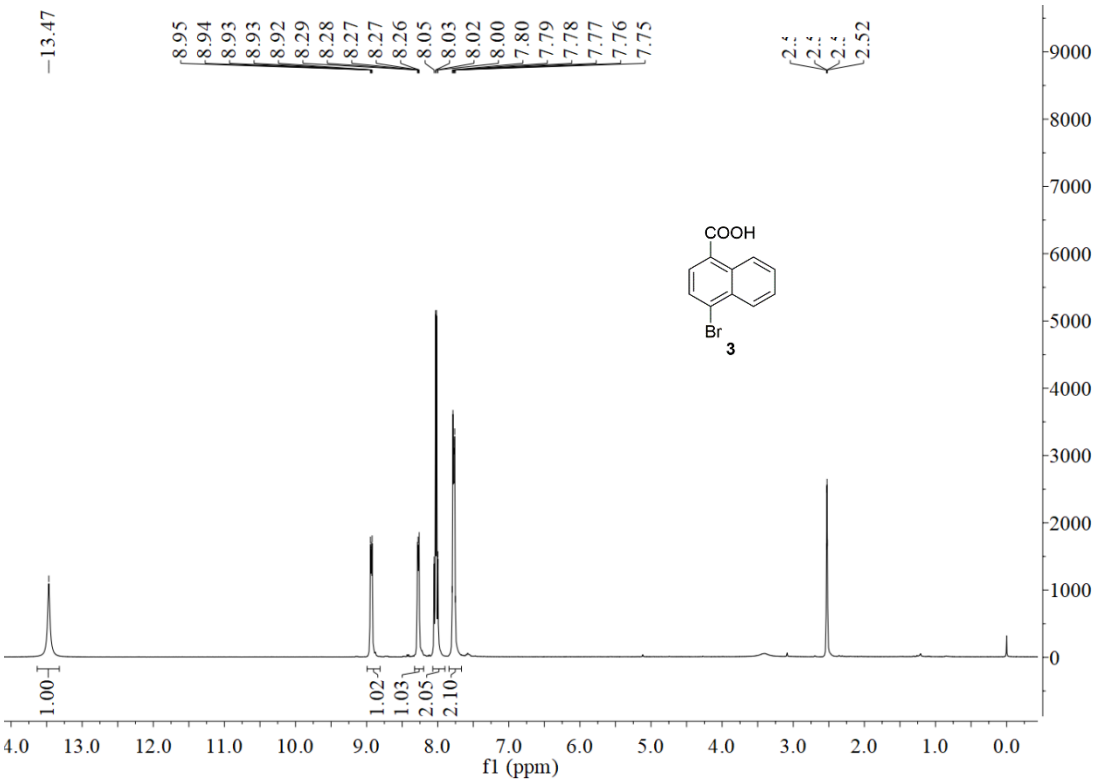
13.47
8.95
8.94
8.93
8.93
8.92
8.29
8.28
8.27
8.27
8.26
8.05
8.03
8.02
8.00
7.80
7.79
7.78
7.77
7.76
7.75
2.52
COOH
Br
3
1.00
1.02
1.03
2.05
2.10
f1 (ppm)

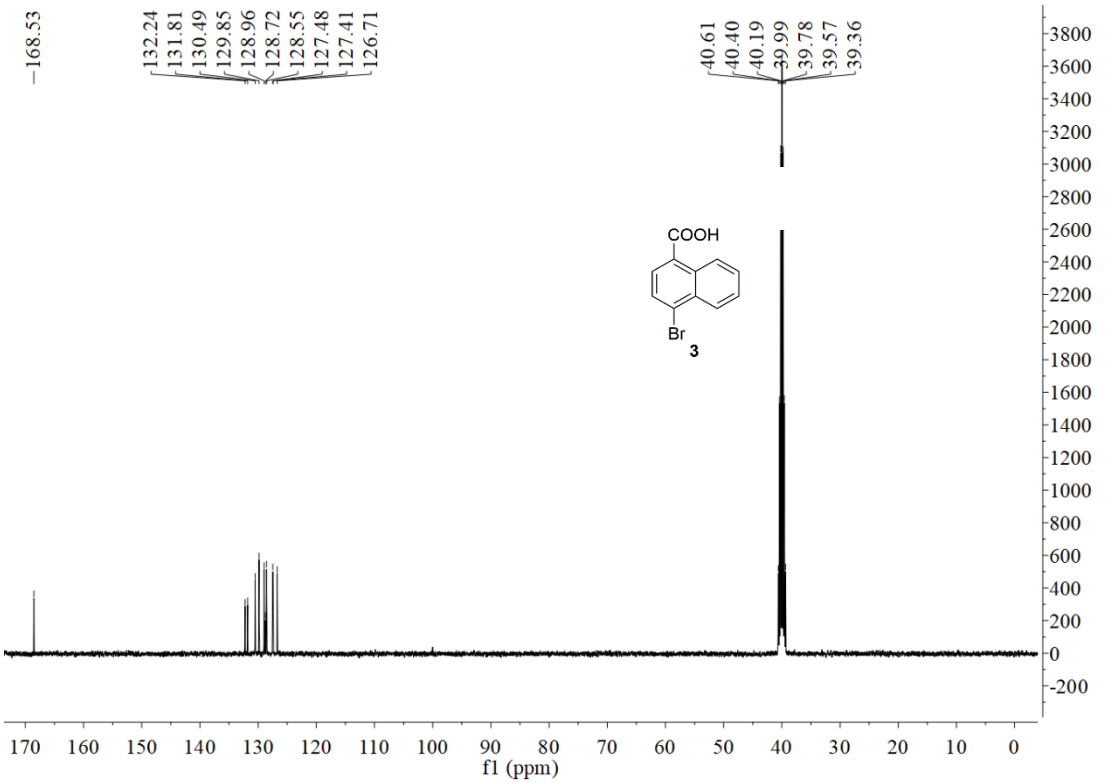
168.53
132.24
131.81
130.49
129.85
128.96
128.72
128.55
127.48
127.41
126.71
40.61
40.40
40.19
39.99
39.78
39.57
39.36
COOH
Br
3
f1 (ppm)

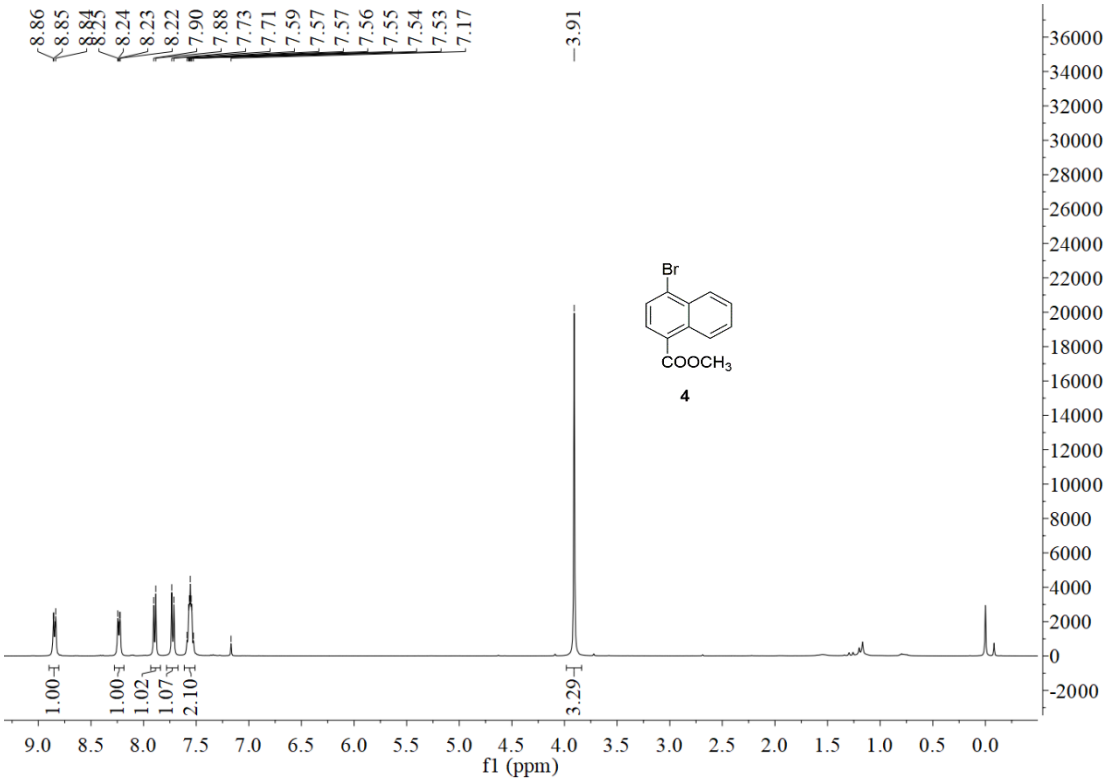
8.86
8.85
8.84
8.25
8.24
8.23
8.22
7.90
7.88
7.73
7.71
7.59
7.57
7.57
7.56
7.55
7.54
7.53
7.17
3.91
Br
COOCH3
4
1.00
1.00
1.02
1.07
2.10
3.29
f1 (ppm)

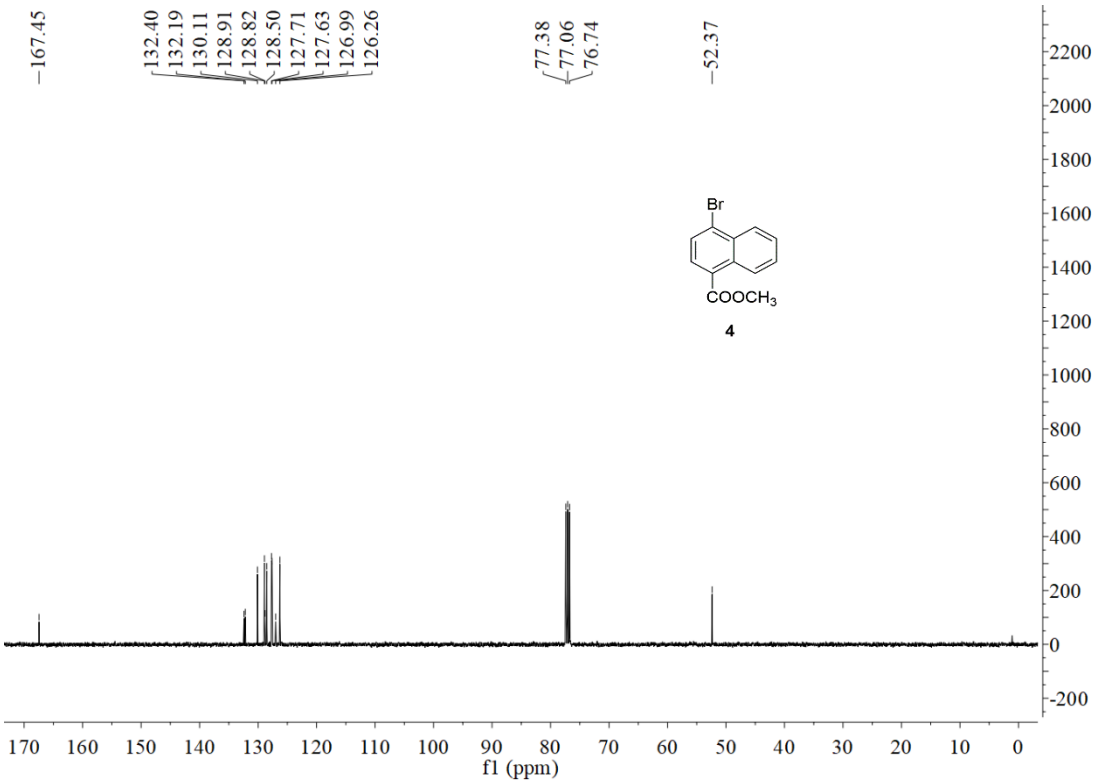
167.45
132.40
132.19
130.11
128.91
128.82
128.50
127.71
127.63
126.99
126.26
77.38
77.06
76.74
52.37
Br
COOCH3
4
f1 (ppm)

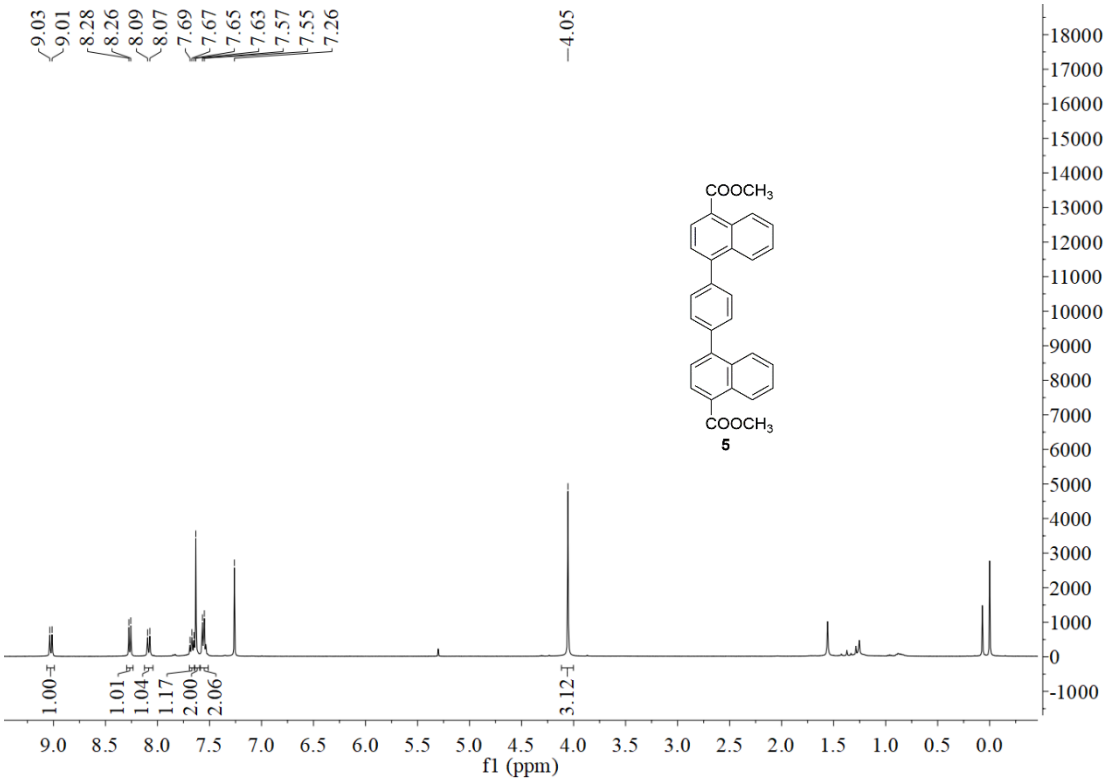
9.03
9.01
8.28
8.26
8.09
8.07
7.69
7.67
7.65
7.63
7.57
7.55
7.26
4.05
COOCH3
COOCH3
5
1.00
1.01
1.04
1.17
2.00
2.06
3.12
f1 (ppm)

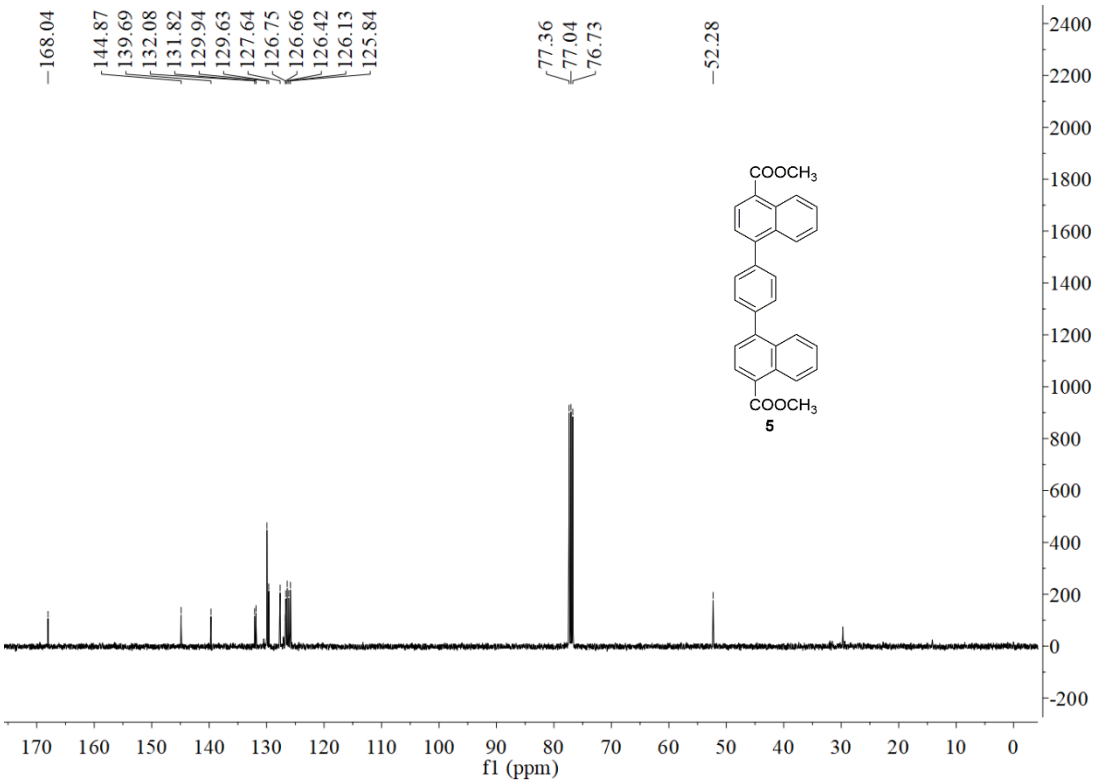
168.04
144.87
139.69
132.08
131.82
129.94
129.63
127.64
126.75
126.66
126.42
126.13
125.84
77.36
77.04
76.73
52.28
COOCH3
COOCH3
5
f1 (ppm)

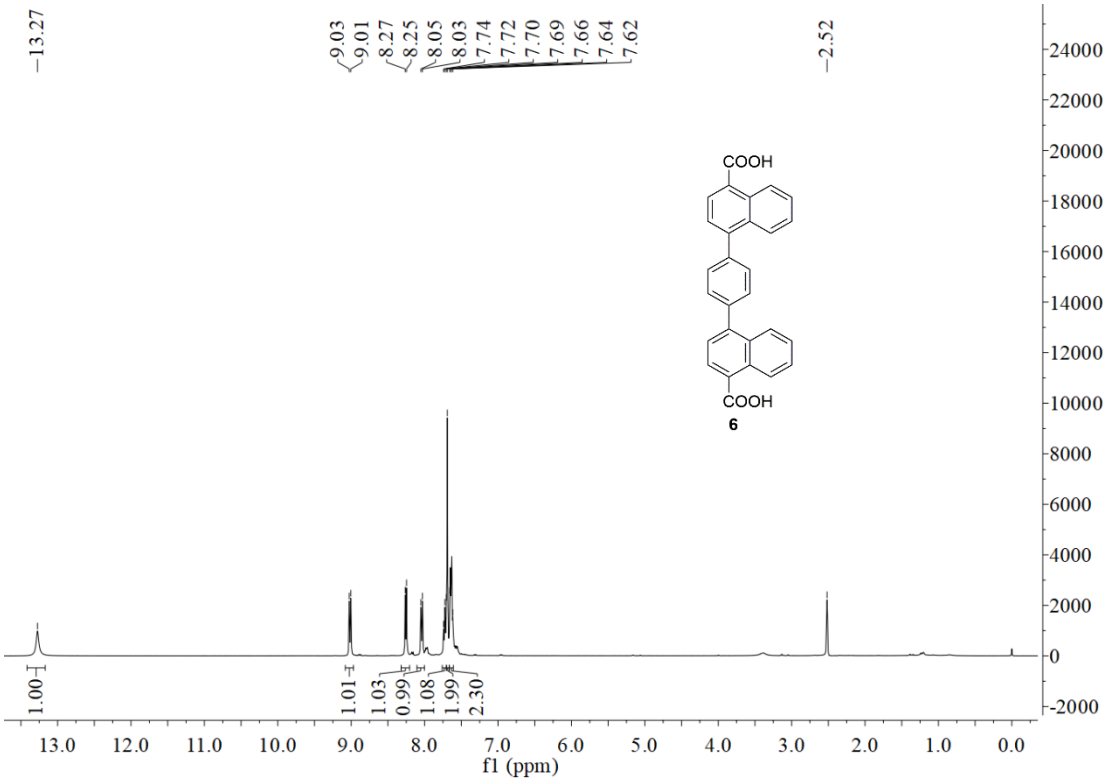
13.27
9.03
9.01
8.27
8.25
8.05
8.03
7.74
7.72
7.70
7.69
7.66
7.64
7.62
2.52
COOH
COOH
6
1.00
1.01
1.03
0.99
1.08
1.99
2.30
f1 (ppm)

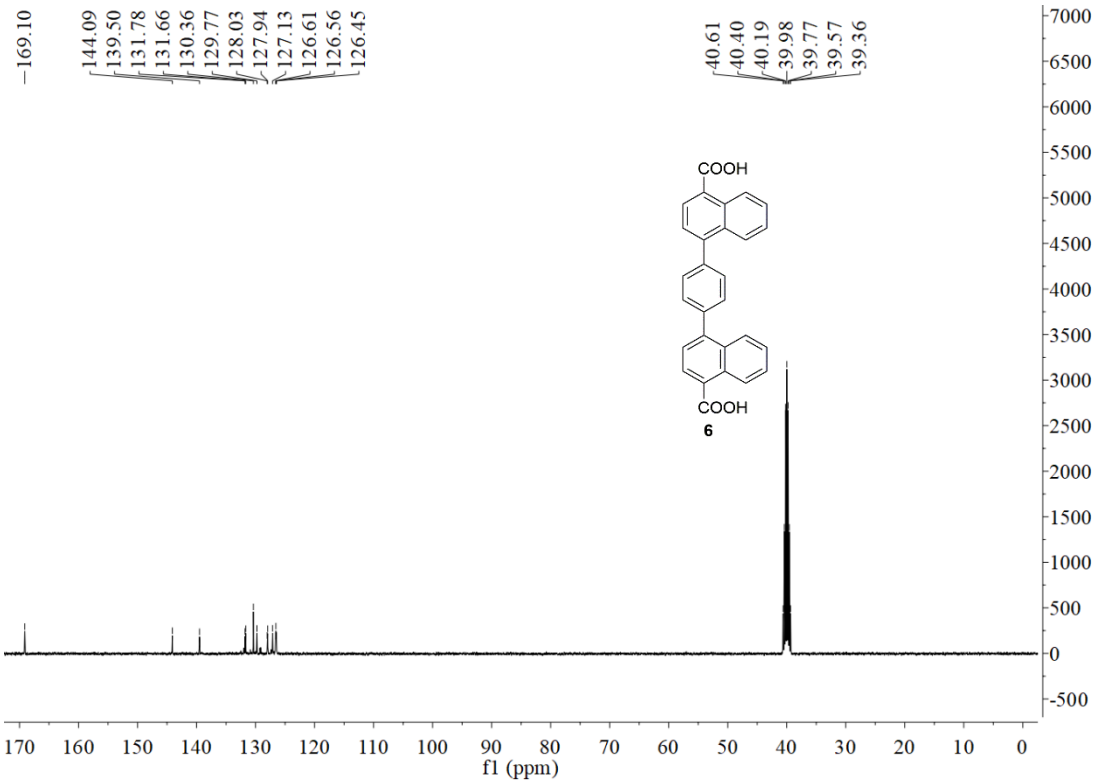

Table 2 Crystal data and structure refinement for ligand.

Identification code	Ligand
Empirical formula	$C_{38}H_{36}N_2O_6$
Formula weight	616.69
Temperature/K	113.15
Crystal system	monoclinic
Space group	C2/c
a/Å	23.369(5)
b/Å	7.7632(16)
c/Å	17.150(3)
α/°	90
β/°	90.52(3)
γ/°	90
Volume/Å^3	3111.1(11)
Z	4
ρ_{calc}g/cm^3	1.317
μ/mm^{-1}	0.089
F(000)	1304.0
Crystal size/mm^3	0.2 × 0.18 × 0.12
Radiation	MoKα (λ = 0.71073)
2Θ range for data collection/°	3.486 to 55.752
Index ranges	$-30 \le h \le 30$, $-9 \le k \le 10$, $-16 \le l \le 22$

Reflections collected	15041
Independent reflections	3708 [R_{int} = 0.0698, R_{sigma} = 0.0582]
Data/restraints/parameters	3708/0/220
Goodness-of-fit on F^2	1.087
Final R indexes [I>=2σ (I)]	R_1 = 0.0630, wR_2 = 0.1336
Final R indexes [all data]	R_1 = 0.0927, wR_2 = 0.1499
Largest diff. peak/hole / e $Å^{-3}$	0.24/-0.23

Table 3 Crystal data and structure refinement for Cu-MOF.

Identification code	**Cu-MOF**
Empirical formula	$C_{34}H_{30}CuN_2O_6$
Formula weight	626.14
Temperature/K	113.1500
Crystal system	triclinic
Space group	P-1
a/Å	10.311(2)
b/Å	12.371(3)
c/Å	14.638(3)
α/°	88.89(3)
β/°	88.16(3)
γ/°	67.68(3)
Volume/$Å^3$	1726.3(7)
Z	2
$\rho_{calc}g/cm^3$	1.205
μ/mm^{-1}	0.675
F(000)	650.0
Crystal size/mm^3	0.2 × 0.18 × 0.12
Radiation	MoKα (λ = 0.71073)
2Θ range for data collection/°	3.558 to 49.998
Index ranges	$-12 \leq h \leq 12$, $-14 \leq k \leq 14$, $-17 \leq l \leq 17$
Reflections collected	16694
Independent reflections	6078 [R_{int} = 0.0644, R_{sigma} = 0.0809]
Data/restraints/parameters	6078/1061/583
Goodness-of-fit on F^2	1.079
Final R indexes [I>=2σ (I)]	R_1 = 0.0933, wR_2 = 0.2510
Final R indexes [all data]	R_1 = 0.1097, wR_2 = 0.2671
Largest diff. peak/hole / e $Å^{-3}$	1.12/-0.75

Table 4 Bond Lengths for Cu-MOF.

Atom	Atom	Length/Å	Atom	Atom	Length/Å
Cu1	Cu1[1]	2.6328(15)	C30	C29	1.3900
Cu1	O1	1.958(4)	C29	C28	1.3900
Cu1	O2[1]	1.972(4)	C29	C32	1.530(9)
Cu1	O3	2.02(2)	C9	C10	1.371(10)
Cu1	O7	2.142(5)	C9	C12	1.492(9)
O1	C1	1.245(8)	C10	C11	1.396(9)
O2	C1	1.261(8)	C12	C13	1.404(10)
O3	C15	1.30(2)	C12	C14	1.379(10)
O4	C15	1.30(3)	C13	C14[2]	1.396(10)
O5	C42	1.33(3)	C15	C16	1.51(2)
O6	C42	1.19(2)	C16	C17	1.3900
O7	C29A	1.247(17)	C16	C25	1.3900
O7	C46	1.270(17)	C17	C18	1.3900
N1	C28A	1.466(13)	C18	C19	1.3900
N1	C46	1.443(13)	C19	C20	1.3900
N1	C47	1.480(13)	C20	C25	1.3900
N1A	C29A	1.448(13)	C20	C21	1.3900
N1A	C30A	1.469(13)	C25	C24	1.3900
N1A	C31A	1.463(13)	C24	C23	1.3900
C1	C2	1.515(8)	C23	C22	1.3900
C2	C3	1.496(11)	C22	C21	1.3900
C2	C3A	1.453(12)	C32	C33	1.3900
C2	C11	1.350(9)	C32	C37	1.3900
C5	C4	1.3900	C33	C34	1.3900
C5	C6	1.3900	C34	C35	1.3900
C4	C3	1.3900	C35	C36	1.3900
C3	C27	1.3900	C35	C42	1.58(3)
C27	C7	1.3900	C36	C37	1.3900
C27	C9	1.518(12)	C36	C41	1.3900
C7	C6	1.3900	C37	C38	1.3900
C5A	C6A	1.3900	C38	C39	1.3900
C5A	C4A	1.3900	C39	C40	1.3900
C6A	C7A	1.3900	C40	C41	1.3900
C7A	C8A	1.3900	O9	C43	1.214(17)
C8A	C3A	1.3900	N3	C43	1.466(13)
C8A	C9	1.388(12)	N3	C44	1.458(13)
C3A	C4A	1.3900	N3	C45	1.450(13)
C8	C26	1.3900	O10	C48	1.152(17)

Table 4 Bond Lengths for Cu-MOF.

Atom	Atom	Length/Å	Atom	Atom	Length/Å
C8	C28	1.3900	N2	C48	1.465(13)
C26	C31	1.3900	N2	C49	1.471(13)
C26	C19	1.541(10)	N2	C50	1.446(13)
C31	C30	1.3900			

[1]1-X,1-Y,-Z; [2]2-X,-Y,1-Z

Table 5 Bond Angles for Cu-MOF.

Atom	Atom	Atom	Angle/°	Atom	Atom	Atom	Angle/°
O1	Cu1	Cu1[1]	84.54(14)	C10	C9	C12	118.2(6)
O1	Cu1	O2[1]	168.37(19)	C12	C9	C27	122.5(8)
O1	Cu1	O3	83.3(6)	C9	C10	C11	121.2(7)
O1	Cu1	O7	93.3(2)	C2	C11	C10	122.1(7)
O2[1]	Cu1	Cu1[1]	83.85(14)	C13	C12	C9	121.5(7)
O2[1]	Cu1	O3	95.1(6)	C14	C12	C9	120.6(6)
O2[1]	Cu1	O7	98.3(2)	C14	C12	C13	117.9(6)
O3	Cu1	Cu1[1]	85.0(6)	C14[2]	C13	C12	120.1(7)
O3	Cu1	O7	97.3(6)	C12	C14	C13[2]	122.0(7)
O7	Cu1	Cu1[1]	176.65(18)	O3	C15	C16	114.9(16)
C1	O1	Cu1	122.9(4)	O4	C15	O3	125(3)
C1	O2	Cu1[1]	122.5(4)	O4	C15	C16	120.2(18)
C15	O3	Cu1	120.8(19)	C17	C16	C15	114.5(6)
C29A	O7	Cu1	116.6(13)	C17	C16	C25	120.0
C46	O7	Cu1	112.7(13)	C25	C16	C15	125.5(6)
C28A	N1	C47	115.0(16)	C16	C17	C18	120.0
C46	N1	C28A	132.4(17)	C19	C18	C17	120.0
C46	N1	C47	112.6(16)	C18	C19	C26	118.7(4)
C29A	N1A	C30A	118.1(17)	C18	C19	C20	120.0
C29A	N1A	C31A	114.0(17)	C20	C19	C26	121.0(4)
C31A	N1A	C30A	127.8(18)	C19	C20	C25	120.0
O1	C1	O2	126.2(5)	C19	C20	C21	120.0
O1	C1	C2	119.0(6)	C25	C20	C21	120.0
O2	C1	C2	114.8(6)	C20	C25	C16	120.0
C3	C2	C1	121.3(7)	C24	C25	C16	120.0
C3A	C2	C1	124.0(8)	C24	C25	C20	120.0
C11	C2	C1	118.4(6)	C23	C24	C25	120.0
C11	C2	C3	119.3(8)	C24	C23	C22	120.0

Table 5 Bond Angles for Cu-MOF.

Atom	Atom	Atom	Angle/°	Atom	Atom	Atom	Angle/°
C11	C2	C3A	116.4(8)	C21	C22	C23	120.0
C4	C5	C6	120.0	C22	C21	C20	120.0
C5	C4	C3	120.0	O7	C29A	N1A	114.7(17)
C4	C3	C2	121.5(9)	C33	C32	C29	117.5(5)
C4	C3	C27	120.0	C33	C32	C37	120.0
C27	C3	C2	118.4(9)	C37	C32	C29	122.3(5)
C3	C27	C9	118.4(9)	C34	C33	C32	120.0
C7	C27	C3	120.0	C35	C34	C33	120.0
C7	C27	C9	121.6(9)	C34	C35	C36	120.0
C27	C7	C6	120.0	C34	C35	C42	115.5(6)
C7	C6	C5	120.0	C36	C35	C42	123.3(6)
C6A	C5A	C4A	120.0	C35	C36	C37	120.0
C7A	C6A	C5A	120.0	C35	C36	C41	120.0
C6A	C7A	C8A	120.0	C37	C36	C41	120.0
C7A	C8A	C3A	120.0	C36	C37	C32	120.0
C9	C8A	C7A	118.6(10)	C38	C37	C32	120.0
C9	C8A	C3A	121.2(10)	C38	C37	C36	120.0
C8A	C3A	C2	119.5(9)	C37	C38	C39	120.0
C4A	C3A	C2	120.1(9)	C38	C39	C40	120.0
C4A	C3A	C8A	120.0	C41	C40	C39	120.0
C3A	C4A	C5A	120.0	C40	C41	C36	120.0
C26	C8	C28	120.0	O5	C42	C35	112.7(18)
C8	C26	C31	120.0	O6	C42	O5	125(3)
C8	C26	C19	120.3(5)	O6	C42	C35	122(2)
C31	C26	C19	119.7(5)	O7	C46	N1	127(2)
C30	C31	C26	120.0	C44	N3	C43	113.4(16)
C31	C30	C29	120.0	C45	N3	C43	118.5(16)
C30	C29	C28	120.0	C45	N3	C44	128.1(17)
C30	C29	C32	121.1(5)	O9	C43	N3	118.8(19)
C28	C29	C32	118.6(5)	C48	N2	C49	117.0(18)
C29	C28	C8	120.0	C50	N2	C48	120.7(18)
C8A	C9	C12	123.1(8)	C50	N2	C49	122(2)
C10	C9	C27	118.6(8)	O10	C48	N2	121(2)
C10	C9	C8A	117.6(8)				

[1]1-X,1-Y,-Z; [2]2-X,-Y,1-Z

1 O. V. Dolomanov, L. J. Bourhis, R. J. Gildea, J. A. K. Howard and H. J. Puschmann, *Appl.Cryst.*, 2009, **2**, 339.
2 G. M. Sheldrick, University of Göttingen, *Germany*, 1997.
3 S. Øien-Ødegaard, B. Bouchevreau, K. Hylland, L. Wu, R. Blom, C. Grande, U. Olsbye, M. Tilset and K. P. Lillerud, *Inorg. Chem.,* 2016, **55**, 1986.